Published November 18, 2002

JCB Article

Membrane proximal lysosomes are the major vesicles responsible for calcium-dependent exocytosis in nonsecretory cells

Jyoti K. Jaiswal,[1] Norma W. Andrews,[2] and Sanford M. Simon[1]

[1]Laboratory of Cellular Biophysics, Rockefeller University, New York, NY 10021
[2]Section of Microbial Pathogenesis and Department of Cell Biology, Yale University School of Medicine, New Haven, CT 06520

Similar to its role in secretory cells, calcium triggers exocytosis in nonsecretory cells. This calcium-dependent exocytosis is essential for repair of membrane ruptures. Using total internal reflection fluorescence microscopy, we observed that many organelles implicated in this process, including ER, post-Golgi vesicles, late endosomes, early endosomes, and lysosomes, were within 100 nm of the plasma membrane (in the evanescent field). However, an increase in cytosolic calcium led to exocytosis of only the lysosomes. The lysosomes that fused were predominantly predocked at the plasma membrane, indicating that calcium is primarily responsible for fusion and not recruitment of lysosomes to the cell surface.

Introduction

Calcium-dependent exocytosis is responsible for key stimulatory events such as neurotransmitter release and hormone secretion, whereas constitutive exocytosis is responsible for the delivery of newly synthesized membrane proteins to the plasma membrane and for the release of extracellular proteins (Palade, 1975). Although all cells exhibit constitutive exocytosis, only recently has it become evident that an increase in intracellular free calcium triggers exocytosis even in the nonspecialized secretory (nonsecretory) cells (Chavez et al., 1996; Coorssen et al., 1996; Ninomiya et al., 1996). Calcium-induced exocytosis in nonsecretory cells is important for the repair of ruptured plasma membrane (McNeil and Steinhardt, 1997), a process proposed to be utilized by intracellular pathogens for the purpose of invasion (Ayala et al., 2001; Andrews, 2002).

Unlike the specialized secretory cells, the cellular and molecular details of calcium-dependent exocytosis in nonsecretory cells are still poorly understood. The lack of consensus regarding the cellular compartment responsible for calcium-regulated exocytosis in nonsecretory cells has been an important hurdle in deciphering further details of this process. On one hand, it has been proposed that specialized synaptic-like vesicles are responsible for the calcium-regulated exocytosis in CHO fibroblasts (Chavez et al., 1996); on the other hand, organelles such as endosomes (Eddleman et al., 1998), Golgi-derived vesicles (Togo et al., 1999), and lysosomes (Rodriguez et al., 1997) have been claimed to be the vesicles responsible for this process.

Calcium influx triggered by membrane damage leads to lysosomal exocytosis in a variety of mammalian cells (Reddy et al., 2001). Exocytosis of lysosomes has also been observed in response to the increase in cytosolic calcium caused by invading pathogens such as *Trypanosoma cruzi* (Caler et al., 1998, 2000) and *Neisseria* (Ayala et al., 2001). Nonetheless, it is still unresolved whether only one or various organelles in nonsecretory cells undergo calcium-regulated exocytosis. Furthermore, obstruction of kinesin- and myosin-driven vesicular transport (Bi et al., 1997) or of actin depolymerization (Miyake et al., 2001) negatively affects the calcium-dependent exocytosis, thereby inhibiting membrane resealing in nonsecretory cells. Thus, it also remains to be elucidated if the role of calcium is to trigger exocytosis of vesicles that are docked at the plasma membrane, or if calcium is responsible for the long range movement, tethering or docking of vesicles at the site of fusion. To address these questions it is important to identify and observe, in situ, the behavior of calcium regulated exocytic compartments in nonsecretory cells.

Total internal reflection fluorescence microscopy (TIR-FM)* offers the ability to visualize events occurring near the cell

The online version of this article contains supplemental material.

Address correspondence to Sanford M. Simon, Laboratory of Cellular Biophysics, Rockefeller University, Box 304, 1230 York Ave., New York, NY 10021. Tel.: (212) 327-8130. Fax: (212) 327-7543. E-mail: simon@rockefeller.edu

Key words: TIR-FM; CD63; dextran; VAMP7; Synaptotagmin VII

*Abbreviations used in this paper: FM, FK506 modified; LAMP, lysomal-associated membrane protein; NRK, normal rat kidney; TIR-FM, total internal reflection–fluorescence microscopy; VAMP, vesicle-associated membrane protein.

Supplemental Material can be found at:
http://jcb.rupress.org/content/suppl/2002/11/14/jcb.200208154.DC1.html

Published November 18, 2002

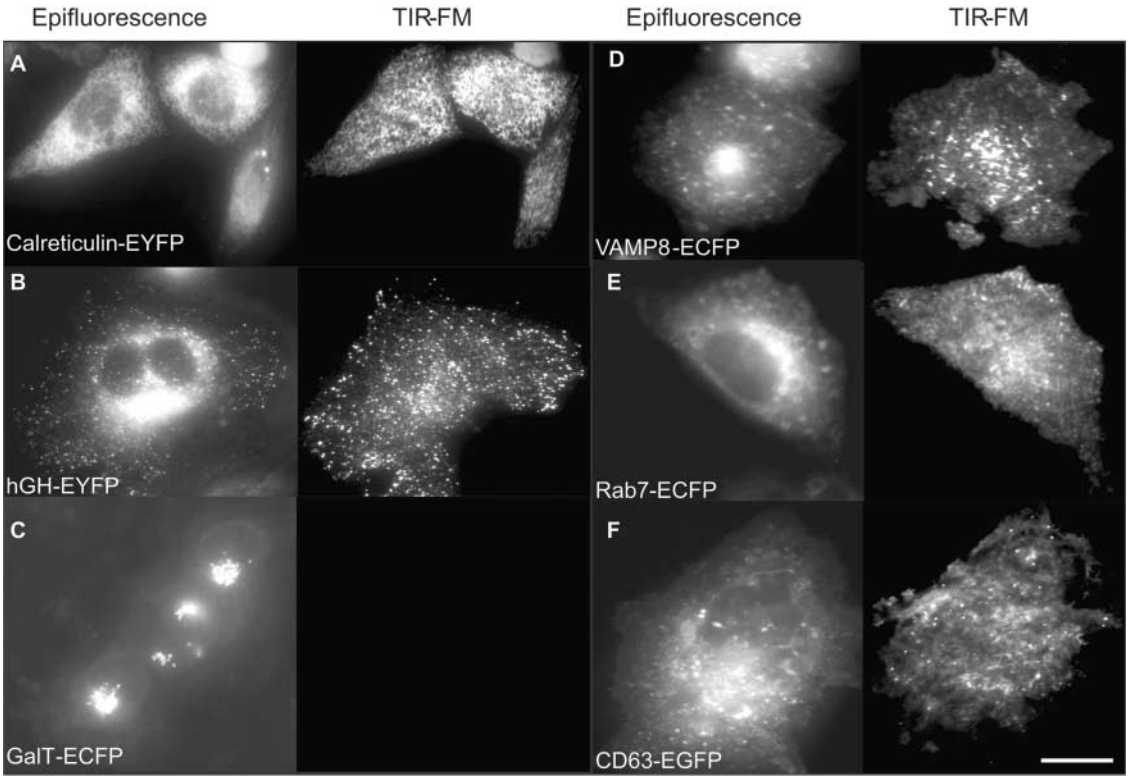

Figure 1. **Distribution of cellular organelles in the evanescent field.** CHO cells were transiently transfected with (A) Calreticulin-EYFP; (B) hGH-EGFP; (C) GalT-ECFP; (D) VAMP8-ECFP; (E) Rab7-ECFP; and (F) CD63-EGFP and imaged using epifluorescence (left) and TIR-FM (right). TIR-FM visualizes the structures that are within 100 nm of the plasma membrane. Note that GalT-ECFP staining (C) shows a total absence of the Golgi apparatus near the plasma membrane. Bar, 10 μm.

surface with a high signal-to-noise ratio (Axelrod, 1981). Earlier work from our and other laboratories has shown that this is a powerful technique for the study of exocytosis (Schmoranzer et al., 2000). Here we have used TIR-FM to study, in live cells, the behavior of fluorescently labeled Golgi apparatus, Golgi-derived vesicles, ER, early endosomes, late endosomes, and lysosomes in response to calcium stimulation. Lysosomes were the only organelles we observed to undergo calcium- induced exocytosis in a variety of nonsecretory cells. Calcium primarily triggered the exocytosis of a pool of lysosomes that were immediately apposed and appear docked to the plasma membrane.

Results

Several organelles are present adjacent to the plasma membrane

Different organelles were visualized by expressing fluorescently tagged reporter proteins in living cells (Fig. 1; Table I). The endoplasmic reticulum was labeled with a fusion protein of YFP and calreticulin (EYFP-ER; CLONTECH Laboratories, Inc.), and the Golgi apparatus was labeled with a fusion protein of CFP and human beta 1,4-galactosyltransferase (GalT-ECFP; Llopis et al., 1998; Zaal et al., 1999). For labeling post-Golgi vesicles, we expressed a fusion protein containing EGFP fused to the NH_2 terminus of human growth hormone containing four FK506 modified (FM) binding domains (EGFP-FM4-hGH; Rivera et al., 2000). The FM domains have been shown to cause aggregation of the newly synthesized fusion protein in the ER. When cells are treated with a ligand that specifically binds the FM domain, the fusion protein disaggregates, becoming free to exit the ER. The disaggregated protein then traverses the constitutive secretory pathway, passing via Golgi into post Golgi vesicles before being exocytosed (Rivera et al., 2000). Early endosomes were labeled with ECFP fused to the COOH terminus of the v-SNARE vesicle-associated membrane pro-

Table I. **Fluorescent tags used to mark the various cellular compartments**

Compartment	Fluorescent Tag(s)	Reference
ER	pEYFP-ER	CLONTECH Laboratories Inc.
Golgi apparatus	pECFP-Golgi	Llopis et al., 1998
Post-Golgi vesicles	H-EGFP	Rivera et al., 2000
Early endosomes	VAMP8-ECFP	Nagamatsu et al., 2001
Late endosomes	Rab7-ECFP	Barbero et al., 2002
Lysosomes	Synaptotagmin VII-EGFP; LAMP1-EGFP; CD63-EGFP; VAMP7-ECFP; dextrans	Martinez et al., 2000; Blott et al., 2001

Published November 18, 2002

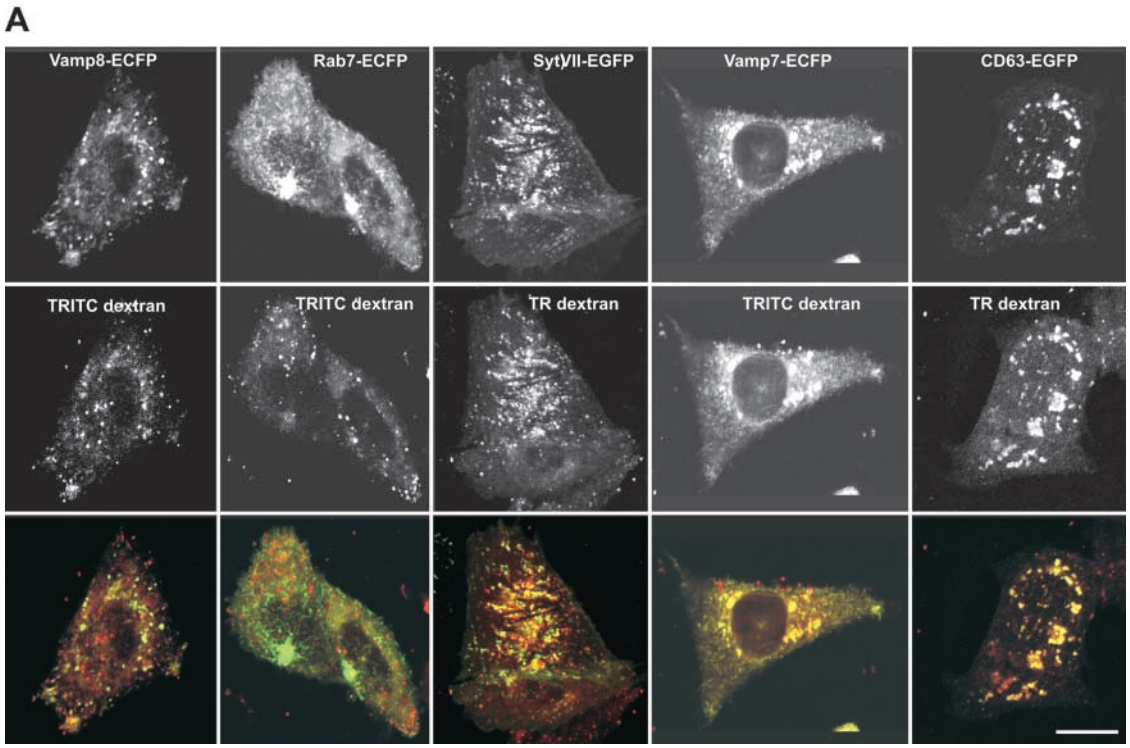

Figure 2. **Lysosomes are located within 100 nm of the plasma membrane in several cell types.** (A) Long-term loading with dextran specifically labels the lysosome. Endocytic compartments of CHO cells transiently transfected with VAMP-ECFP, Rab7-ECFP, SytVII-EGFP, VAMP7-ECFP, and CD63-EGFP were loaded for 2 h with TRITC dextran or Texas red dextran followed by a 5-h chase in dextran-free media. The images represent 0.4 μm thick Z confocal sections which contained the maximum number of labeled vesicles. (B) Lysosomes are detected by TIR close to the plasma membrane. CHO cells transiently transfected with SytVII-EGFP, Lamp1-EGFP, and VAMP7-ECFP were imaged using TIR-FM. Each of these lysosome specific markers were found to be present within the evanescent field. (C) Lysosomes are detected by TIR close to the plasma membrane in several cell types. Lysosomes in NIH3T3 fribroblasts, WM239 melanoma cells, HeLa cells, MDCK epithelial cells, and murine embryonic primary fibroblasts were loaded with FITC dextran as in Fig. 1, and the cells were visualized using TIR-FM. Bar, 10 μm.

tein (VAMP)8-ECFP (Nagamatsu et al., 2001), whereas late endosomes were labeled with ECFP fused to the NH_2-terminal of Rab7 (Rab7-ECFP; Barbero et al., 2002).

For labeling the lumen and the membrane of lysosomes two complementary approaches were used. The membrane was labeled by transiently expressing fluorescent reporter proteins including Synaptotagmin VII-EGFP (Martinez et al., 2000), lysosomal associated membrane protein (LAMP)1-EGFP (Kornfeld and Mellman, 1989), CD63-EGFP (Blott et al., 2001), and VAMP7-ECFP (Advani et al., 1999). For labeling the lysosomal lumen, the entire endocytic pathway was first loaded with fluorescent dextran followed by a chase of 3–10 h. In these conditions, dextran was retained predominantly in the lysosomes (Fig. 2 A). The fluorescent dextran colocalized with VAMP8-ECFP (diagnostic of early endosomes) only shortly after incubation (unpublished data). 3 h after shifting the cells to dextran-free media, no fluorescent dextran colocalized with VAMP8-ECFP, very little colocalized with Rab7-CFP–labeled vesicles (diagnostic of late endosomes), whereas the bulk of dextran colocalized with vesicles labeled with the lysosomal markers Synaptotagmin VII-EGFP, VAMP7-ECFP, and CD63-EGFP (Fig. 2 A).

To study only those fluorescently labeled compartments that are near the plasma membrane, cells were observed using TIR-FM. In TIR-FM, the excitatory evanescent field decays exponentially from the interface of the cell membrane and coverslip, thus illuminating a region 70–120 nm from the plasma membrane (see Materials and methods). Thus, fluorophores that are any further from the plasma membrane are very poorly excited. This allows us not only to monitor the vesicles and organelles near the basal cell membrane with a high signal to noise ratio but also minimize the photo-damage due to laser excitation.

Using epifluorescence and TIR-FM microscopy, we observed that compartments containing calreticulin-EYFP (Fig. 1 A, diagnostic of ER), human growth hormone–EGFP conjugated to four FM domains (Fig. 1 B, diagnostic of post Golgi derived vesicles), VAMP8-ECFP (Fig. 1 D, early endosomes), Rab7-ECFP (Fig. 1 E, late endosomes), and CD63-EGFP (Fig. 1 F, lysosomes), were present both deeper in the cell and within the evanescent field. In contrast, the galactosyl-transferase-ECFP (Fig. 1 C, diagnostic of Golgi apparatus; Sciaky et al., 1997; Llopis et al., 1998; Zaal et al., 1999)-labeled compartments were observed only deeper inside the cell and were not visible in the evanescent field.

With the exception of the lysosomes and Golgi apparatus, all of the other organelles mentioned above, including the endoplasmic reticulum (Lysakowski et al., 1999; Nagata, 2001), post-Golgi vesicles (Schmoranzer et al., 2000) and

Published November 18, 2002

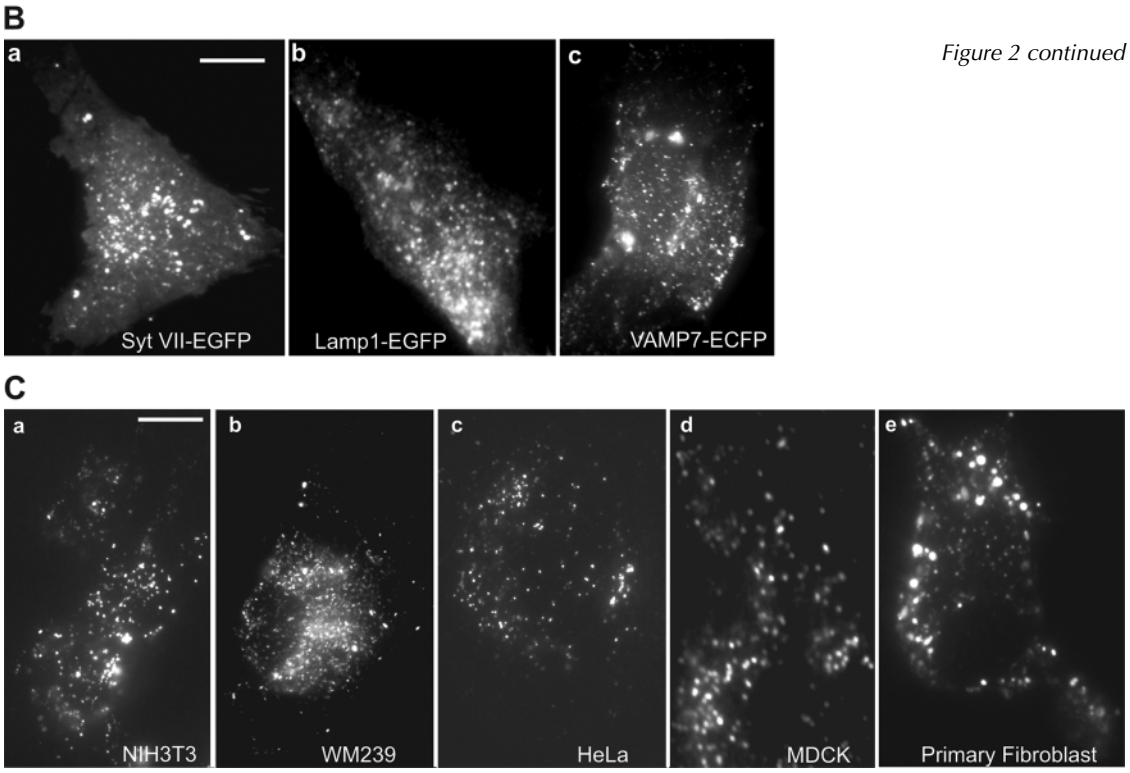

Figure 2 continued

endosomes (Lampson et al., 2001) have been observed within 100 nm from the plasma membrane. Because the existence of a population of lysosomes adjacent to the plasma membrane has not been characterized, we tested if additional lysosomal markers were observed in the evanescent field (Fig. 2 B). With each of the fluorescently tagged lysosomal membrane proteins used, synaptotagmin VII, Lamp1, and VAMP7, we observed a population of vesicles adjacent to the plasma membrane, within the evanescent field (Fig. 2 B). Further, to examine if a peripheral population of lysosomes was typical of only CHO cells, we repeated the experiment in various cell lines (Fig. 2 C). All the cell lines examined (NIH3T3 fibroblasts, WM239 melanoma, MDCK epithelial cells, normal rat kidney (NRK) fibroblasts, HeLa cells, and murine embryonic primary fibroblasts) possessed a fraction of dextran labeled lysosomes adjacent to the plasma membrane.

Increase in calcium triggers exocytosis of lysosomes, but not of other organelles

To assess the effect of calcium on the movement and distribution of the fluorescently tagged compartments in the evanescent field, and on their ability to exocytose, cellular calcium was increased using the calcium ionophore A23187 (10 μM; Bennett et al., 1979). After the ionophore treatment, cells were continuously imaged (at 5–10 frames/s) using TIR-FM. Observations were limited to an interval of $<$10 min, because treatment with the calcium ionophore A23187 often caused cells to round up after longer periods, leading to their disappearance from the evanescent field. Within this interval, the vesicles were analyzed for movement and fusion based on total fluorescence intensity, peak intensity, and the width squared ([width]^2) of the spread of fluorescence. As demonstrated previously (Schmoranzer et al., 2000), movement of a fluorescent vesicle perpendicular to the coverslip alters the excitation by evanescent field, thereby resulting in changes in the fluorescence emission intensity. A fusion event, leading to the delivery of all membrane proteins of a vesicle to the plasma membrane, is determined by two criteria. First, there is an increase in the peak fluorescence intensity and the total fluorescence intensity (as all fluorophores are delivered to the plasma membrane, and hence better excited by the evanescent wave). Second, there is an increase in the width of the spread of fluorescence (as the vesicular membrane proteins diffuses into the plasma membrane; Schmoranzer et al., 2000). Upon fusion the rate at which the (width)^2 of the fluorescence increases is linear with time, the slope of which is equal to the diffusion constant for the membrane protein. If a vesicle lysed, the (width)^2 would increase significantly faster and there would be no net delivery of fluorophores to the plasma membrane.

The organelles and vesicles we examined after stimulation of the cells with calcium ionophore fell into three groups. In one group, the vesicles stopped moving and became stationary adjacent to the membrane, or were stationary during the entire period of observation. In the second group, the vesicles showed synchronous increases and decreases in the total and peak fluorescent intensities, with no significant change in the width. The third group of vesicles showed synchronous increase in total and peak intensities, and a concomitant increase in the width of fluorescence. These results are consistent with the first group of vesicles docking with the plasma membrane but not fusing during the observation period; the second group of vesicles moving in and out of the plane of the evanescent field, without fusing with the plasma membrane; and the third group fusing to the plasma membrane.

Published November 18, 2002

Table II. **Effect of ionophore induced calcium increase on exocytosis of organelles in CHO cells**

Organelle	*n* = cells	Exocytic events (per min) observed in Untreated cells	10 μM A23187- treated cells	Fold increase in rate of exocytosis induced by A23187
ER	*n* = 5	0	0	–
Golgi apparatus	*n* = 4	0	0	–
Post-Golgi vesicles	*n* = 6	6 ± 2	6 ± 2	0
Early endosomes	*n* = 5	0	0	–
Late endosomes	*n* = 6	0	0	–
Lysosomes	*n* = 8	1 ± 1	25 ± 14	25

In untreated cells, we did not observe the Golgi apparatus in the evanescent field ($n = 4$; Fig. 1 C). The endoplasmic reticulum ($n = 5$), early endosomes ($n = 5$), late endosomes ($n = 6$), and lysosomes ($n = 23$) were present in the evanescent field (Fig. 1, A, D, E, and F). Based on the above mentioned criteria, these compartments fell into the first or the second group of vesicles: no exocytosis was observed. Post-Golgi transport vesicles were also seen in the evanescent field ($n = 6$) in CHO cells (Fig. 1 B), which exocytosed at the rate of 6 ± 2/min ($n = 4$). Treatment with calcium ionophore did not affect the rate of fusion of the post-Golgi vesicles. The Golgi apparatus, ER, early endosomes, and late endosomes were never observed to exocytose in the presence or absence of calcium iono-

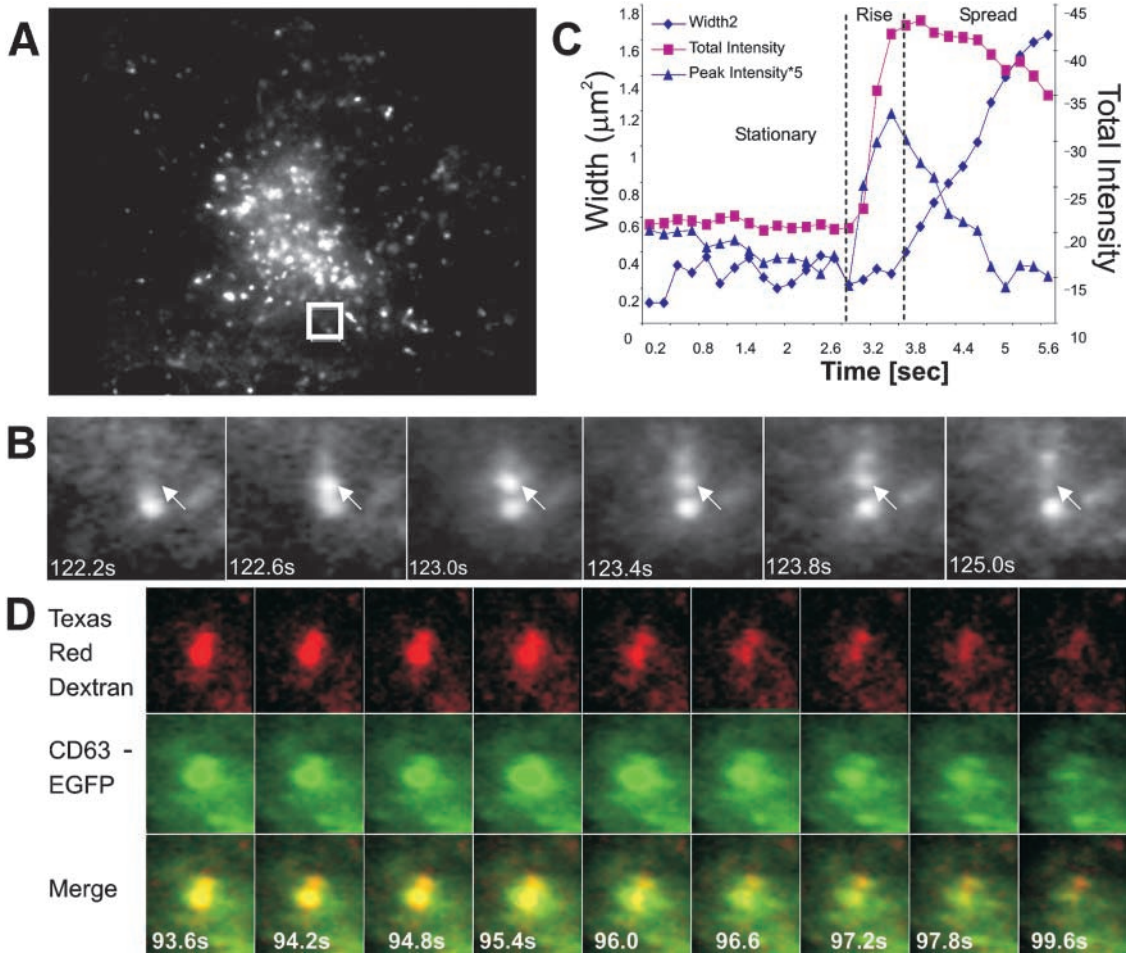

Figure 3. **Lysosomal membrane and lumenal markers confirm that calcium induces exocytosis of lysosomes.** NRK cells labeled with either CD63-EGFP (A–C) or CD63-EGFP (D) and 10 kD Texas red–dextran were treated with 10 μm A23187 ionophore and imaged using TIR-FM. A region from A that shows a cell with CD63-EGFP–labeled lysosomes in the evanescent field. A lysosome that underwent exocytosis has been enlarged in B; the arrow indicates a CD63-EGFP–labeled lysosome that moved into the evanescent field during the period of observation and fused to the plasma membrane. Note that it takes ~3 s for the fluorescence to diffuse out along the membrane. (C) The quantification of the peak, total intensity and (half-width)^2 of the fluorescence for a lysosome that undergoes fusion (the values for peak intensity has been multiplied by a factor of five). The point when lysosome ceased moving before initiation of fusion was used as t = 0. (D) Representative images of a lysosome double labeled for membrane (green; using CD63-EGFP) and lumen (red; Texas red dextran) that underwent calcium-induced fusion. The arrow points to a lysosome that underwent exocytosis. The time stamp represents the time elapsed after the addition of ionophore. Note that the dextran fluorescene (red) diffuses much faster compared with the diffusion of the fluorescence of the membrane marker (green; Video 2).

Published November 18, 2002

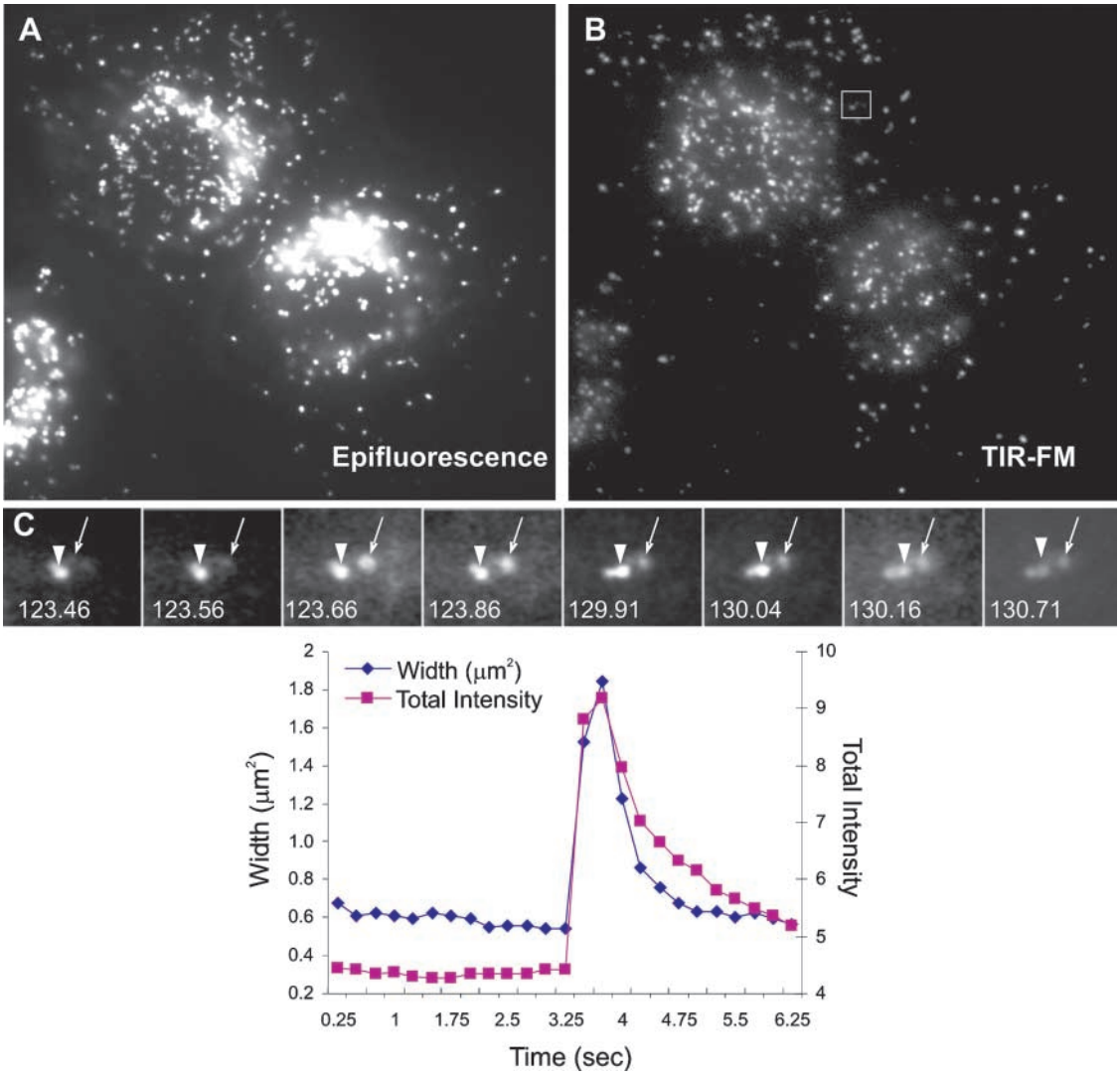

Figure 4. **Characterization of lysosomal exocytosis by monitoring the release of a lumenal marker.** Lysosomes in NRK cells were loaded with FITC dextran and cells were treated with 10 μm A23187 calcium-ionophore. Although the epifluorescence image (A) predominantly demonstrates the perinuclear population of lysosomes, TIR-FM (B) allows identification of lysosomes near the plasma membrane. In response to the addition of calcium ionophore there is a reduction in lysosomal movement and ~7% of the total lysosomes in the evanescent field exocytose (Video 3). (C) Most of the exocytosing lysosomes are predocked (arrowhead), whereas a few recent arrivals (arrow) also exocytose. Time stamp indicates the time elapsed since the addition of ionophore. (D) Quantification of changes in the total intensity and (half-width)^2 of the fluorescence of exocytosing dextran. X-axis represents the time starting from when the lysosome ceased moving before initiation of fusion. Note that the spread phase for dextran (a lumenal marker) is much shorter compared with the spread phase for a CD63-EGFP (a membrane marker; Fig. 3 C).

phore (Table II). Further, calcium affected neither the movement nor the number of any of these organelles in the evanescent field.

The only compartment that exhibited increased exocytosis in response to an increase in calcium was the lysosome (Table II). In contrast to unstimulated cells ($n = 8$) where almost none of the CD63-EGFP labeled lysosomes were observed to undergo exocytosis, after the addition of ionophore, many CD63-labeled lysosomes were visualized fusing with the plasma membrane (Fig. 3, A and B). The total intensity, peak intensity, and the (width)^2 of the fluorescence for one of these fusion events is plotted as a function of time in Fig. 3 C. These data allow us to clearly distinguish three temporal phases, designated as stationary, rise, and spread.

To demonstrate that exocytosing vesicles were bona-fide lysosomes and not biosynthetic transport vesicles carrying newly synthesized CD63-EGFP, or mislocalized protein as a consequence of overexpression, we loaded the lysosomes of CD63-EGFP–transfected cells, as described above, with Texas red–dextran. Most of the CD63-EGFP–labeled vesicles also contained Texas red–dextran (Figs. 2 A and 3 D), and addition of ionophore led to the exocytosis of vesicles containing both fluorophores (Fig. 3 D; Video 2, available at http://www.jcb.org/cgi/content/full/jcb.200208154/DC1). Analysis of cells containing lysosomes loaded with Texas red–dextran showed that none of the lysosomes exocytose in untreated cells. Similar to the CD63-EGFP–transfected cells, after the addition of ionophore, large-scale exocytosis of dextran-loaded lysosomes was observed (Figs.

Published November 18, 2002

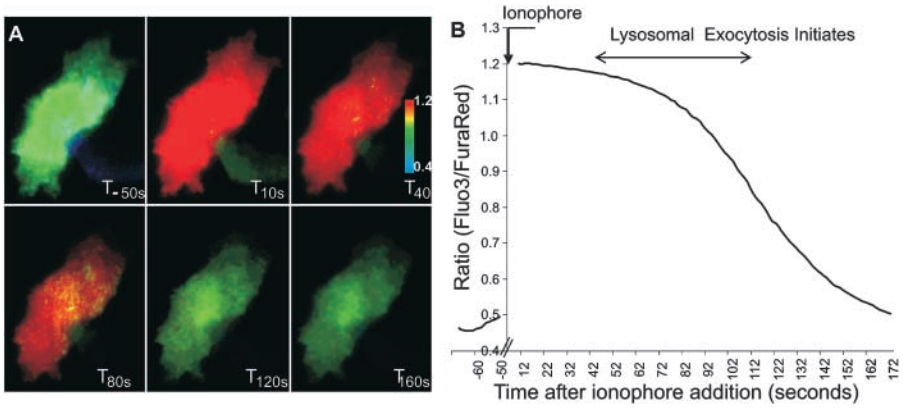

Figure 5. **Lysosomal exocytosis initiates with a delay after the increase in intracellular calcium.** CHO cells were loaded for 20 min with Fluo-3-AM and Fura red–AM, after which 10μm A23187 calcium-ionophore was added (T_{0s}) and the cells were imaged using TIR-FM. The cells were illuminated using 488 nm laser light and the emission from both the two dyes was simultaneously and continuously imaged as described in Materials and methods. The images were subtracted for background and pseudo colored ratio images of Fluo-3/Fura red were generated. (A) Selected ratio images of a cell at various time points after the addition of ionophore. Within 10 s after the addition of ionophore, calcium reached the peak value, which dropped to prestimulatory levels over next 120 s. The pseudo color code represents increasing ratio (hence calcium) from blue to red (B) The trace of ratio of Fluo-3/Fura red emission intensities before and after the addition of ionophore. Note that in all the cell lines imaged (n = 42 cells), lysosomal exocytosis was initiated during the phase when submembrane calcium level started to decline, after the initial ionophore induced increase.

2 C, e, and 4, A–D; Videos 1 and 3, available at http://www.jcb.org/cgi/content/full/jcb.200208154/DC1). Unlike CD63-EGFP, which is a membrane protein, dextran is present in the lumen of the lysosome. Thus, after fusion, whereas CD-63 diffuses in a two-dimensional plane, dextran diffuses in three dimensions, and hence at a much faster rate. This is reflected in the $(\text{width})^2$ and total intensity plots of the fluorescence of the exocytosing dextran (Fig. 4 D), which shows a much faster diffusion of fluorescence compared to diffusion of CD63-EGFP fluorescence (Fig. 3 C). Using the above quantitative criterion established for vesicle fusion (Schmoranzer et al., 2000), we ascertained that these events were not lysis, but genuine membrane fusion events.

Extent of lysosomal exocytosis is sensitive to cell type and calcium level

To examine if calcium induced exocytosis of lysosomes was unique to CHO and NRK cells, we loaded HeLa, WM239 (melanoma), and murine embryonic primary fibroblast (primary isolates) cells with fluorescent dextran (Fig. 2 C). The cells were then treated with 10 μM calcium ionophore. The extent of lysosomal exocytosis varied depending on the cell type used and also on the amount of calcium in the media (Table III). Among all the cell lines tested, calcium increase induced maximum lysosomal exocytosis in the primary fibroblasts (see Fig. 6 B; Table III; Video 1). The weakest response to ionophore induced calcium increase was in HeLa cells. In these cells, the calcium ionophore-induced lysosomal exocytosis was barely detectable until the extracellular calcium was raised to 5 mM or 10 mM, at which point the rate of lysosomal exocytosis was similar to that in CHO cells in media containing 1.2 mM extracellular calcium (Table III).

Within the first 35 s of the addition of ionophore, no lysosomal exocytosis was seen in any of the cell lines tested (n = 42). To test if this delayed response was related to the kinetics of calcium elevation or a later step, we monitored the time course of ionophore-induced increase in calcium near the plasma membrane using TIR-FM (Fig. 5). Fluo-3-AM and Fura red–AM fluorescence emission ratio imaging has previously been used to monitor cytosolic calcium levels (Floto et al., 1995). Thus, we loaded CHO cells with both the dyes and simultaneously imaged their emission using a split optics setup (described in Materials and methods). Within 10 s of ionophore addition, the free calcium concentration near the plasma membrane reached the maximum value, and then declined to below the prestimulation levels over the next 150 s (Fig. 5, A and B). In contrast, the time elapsed to the first observed lysosomal exocytosis ranged from 35 to 100 s after the addition of ionophore (n = 42), indicating that under these conditions, there is a time lag between increase in calcium level near the plasma membrane and initiation of lysosomal exocytosis. Once exocytosis was initiated, many more lysosomes fused with the plasma membrane within the next 3–7 min. The lysosomes remaining within the evanescent field after this period (94 ± 1% of the total in CHO cells) did not undergo exocytosis. Further ad-

Table III. **Cell-type dependence of the extent of calcium induced lysosomal exocytosis**

Cell type	Treatment	Fraction of peripheral lysosomes that exocytose
		n = cells
NRK	A23187 with 1.2 mM extracellular calcium	7 ± 1% (n = 21)
CHO	A23187 with 1.2 mM extracellular calcium	5 ± 1% (n = 8)
WM239	A23187 with 1.2 mM extracellular calcium	<2% (n = 4)
HeLa	A23187 with 1.2 mM or 2 mM extracellular calcium	0% (n = 8)
HeLa	A23187 with 5 mM or 10 mM extracellular calcium	4 ± 0.8% (n = 4)
Murine embryonic primary fibroblast	A23187 with 1.2 mM extracellular calcium	24 ± 6% (n = 6)

Published November 18, 2002

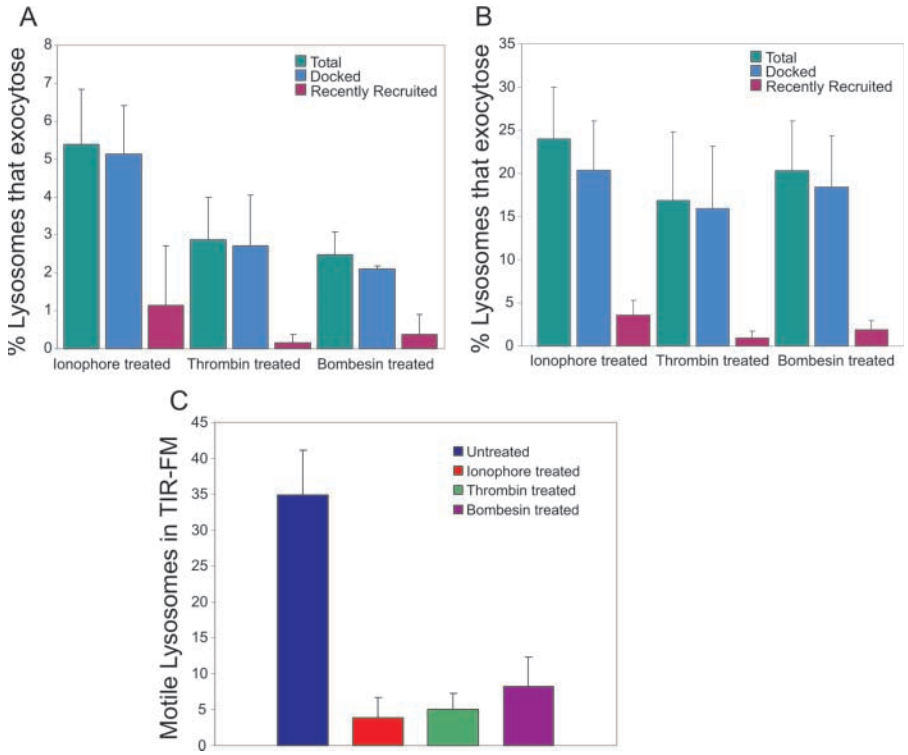

Figure 6. **Predocked lysosomes are primarily responsible for calcium induced exocytosis.** Cells loaded with fluorescent dextran were treated with 10 μM calcium-ionophore, 0.2 U/ml thrombin, or 20 nM bombesin. The cells were continuously imaged using TIR-FM. A frame-by-frame analysis was performed to identify the exocytosing and motile lysosomes. In the case of both (A) CHO cells and (B) murine embryonic primary fibroblasts, treatment with calcium ionophore, thrombin and bombesin led to lysosomal exocytosis. The murine embryonic primary fibroblasts showed approximately fivefold greater exocytosis than the CHO cells. (C) Increase in calcium caused both by ionophore and IP3 agonists, bombesin and thrombin led to a reduced motility of the lysosomes in the evanescent field. (Lysosomes that appeared or disappeared from the evanescent field, or moved >1 μm within the evanescent field were classified as motile.)

dition of the calcium ionophore A23187 had no effect on this residual population of lysosomes.

To test whether a physiological stimulus that mobilized calcium from intracellular stores would also lead to lysosomal exocytosis, cells were treated with thrombin (0.2 U/ml) or bombesin (20 nM). Bombesin and thrombin are agonists of surface receptors linked to PLC and phosphoinositide hydrolysis, resulting in IP3 formation and mobilization of Ca^{2+} from intracellular stores (Neylon et al., 1992; Van Lint et al., 1993). Both these agents led to exocytosis of dextran-loaded lysosomes in CHO and in murine embryonic primary fibroblasts. Treatment with calcium channel agonists gave a similar result to the ionophore: there was a significantly higher lysosomal exocytosis in primary fibroblasts (16 to 17%) than in CHO cells (2 to 3%; Fig. 6, compare A and B).

Calcium induces exocytosis of lysosomes present at the plasma membrane

Based on the spatial localization, there appears to be two populations of lysosomes in mammalian cells which can be distinguished in epifluorescence and TIR fluorescence microscopy (Figs. 1 and 4). Although many lysosomes are present in the perinuclear region near the microtubule-organizing center, a smaller number of lysosomes are present as a docked or motile population near the plasma membrane. Because in CHO cells there was a 35–100-s delay between the increase in the intracellular calcium concentration near the plasma membrane and lysosomal exocytosis, we examined the possibility that calcium increase leads to the recruitment of lysosomes from the deeper perinuclear regions of the cells to the sites of exocytosis at the plasma membrane.

To identify which of the two populations of lysosomes, perinuclear or plasma membrane apposed, was responsible for exocytosis we tracked individual lysosomes in CHO cells and murine embryonic primary fibroblasts. Both in the CHO cells (Fig. 6 A) and primary fibroblasts (Fig. 6 B), >80% of the lysosomes that exocytosed were present in the evanescent field before the increase in cytosolic calcium. Moreover, whereas in untreated CHO cells 35% of the lysosomes present in the evanescent field were motile, addition of calcium ionophore led to a rapid loss of movement of these lysosomes ($n = 21$) (Fig. 6 C). Increase in calcium did not lead to a significant increase in the recruitment of lysosomes to the vicinity of the plasma membrane, but instead (due to exocytosis), over a period of 5–10 min there was a 4 ± 1% decrease in the total number of lysosomes in the evanescent field. Further, the majority of lysosomes in CHO cells (210 out of 270, [~81%]) that underwent exocytosis did not move before undergoing fusion. Similar observations were made with the primary fibroblasts. Thus, addition of the calcium ionophore seems to cause the exocytosis of lysosomes that are apparently docked at the plasma membrane.

Discussion

The use of TIR-FM enabled us to visualize the steady state and calcium-induced submembrane movement, docking, and fusion of intracellular compartments to the plasma membrane. We found that calcium ionophore A23187 induced increase in calcium did not cause exocytosis of Golgi, ER, early, or late endosomes, and did not lead to an increase in exocytosis of post-Golgi vesicles. The absence of an effect of calcium on exocytosis of early endosomes is in agreement with the previously reported absence of an affect of calcium increase on transferrin recycling (Rodriguez et al., 1997). On the other hand, absence of an effect of calcium on exocy-

tosis of Golgi and Golgi-derived vesicles is contrary to the proposed role of Golgi derived compartments in Ca^{2+}-induced exocytosis in fibroblasts (Togo et al., 1999).

An increase in calcium caused either by the calcium ionophore A23187 or by the IP3-dependent calcium channel agonists thrombin and bombesin, led to exocytosis of lysosomes. Using dual-color live-cell imaging to simultaneously visualize the presence of membrane and lumenal markers, we found that calcium induced the exocytosis of both lysosomal membrane and lumenal markers (Fig. 3 D; Video 2). Identification of lysosomes as the vesicles responsible for A23187-dependent exocytosis is in agreement with the earlier reports of calcium-induced lysosomal exocytosis in fibroblast and epithelial cells (Reddy et al., 2001). It is also in agreement with the size (0.4–1.5 μm) and density (~1.12 g/ml) reported for a calcium-regulated exocytic compartment present in CHO cells (Chavez, et al., 1996; Ninomiya et al., 1996).

Most of the lysosomes that underwent calcium-dependent exocytosis are those that are present near the plasma membrane (Fig 6, A and B; Videos 1 and 3). Moreover, an increase in calcium also led to a reduction in the fraction of motile lysosomes in the evanescent field (Fig. 6 C). Thus, similar to the calcium-regulated exocytic vesicles present in specialized secretory cells, in nonsecretory cells, calcium appears to be primarily responsible for the fusion rather than recruitment of lysosomes to the plasma membrane. Although in CHO and other cell lines only a small proportion of the membrane proximal lysosomes underwent fusion, in primary fibroblasts, this number was significantly higher, reaching ~24% (Table III). Because exocytosis of lysosomes has been implicated in the process of membrane repair (Reddy et al., 2001), the cell-type–specific differences in the extent of lysosomal exocytosis observed here may correspond to the cell-type–specific sensitivity to calcium previously reported in membrane resealing assays (Steinhardt et al., 1994). On the other hand, we cannot exclude the possibility that different cell types differ in their sensitivity to the calcium ionophore. It is important to note that, unlike a rupture in the plasma membrane, treatment with calcium ionophores does not equilibrate the cytosolic calcium with the extracellular calcium (Kendall et al., 1996). Therefore, it remains to be determined if calcium influx during a membrane wound, which results in free intracellular calcium concentrations at the millimolar level, triggers the exocytosis of a larger fraction of the lysosomal population.

A good example of cell lineage-specific differences in the extent of lysosomal exocytosis is provided by the secretory lysosomes of hemopoietic cells, which can correspond to as much as 60% of the total lysosomal population. In hemopoietic cells, secretory lysosomes have the unique ability to store specific secretory proteins in their lysosome-like granules, while maintaining its endocytic and degradative capabilities (Stinchcombe and Griffiths, 1999; Blott and Griffiths, 2002). Our results reveal a remarkable similarity between calcium regulated exocytic vesicles from nonsecretory and those present in specialized secretory cells, in so far that both are peripherally located granule population with lysosomal properties and that they respond to calcium by fusing with the plasma membrane (Marks and Seabra, 2001; Blott and Griffiths, 2002).

Calcium-induced exocytosis is important in the repair of membrane rupture and the invasion of cells by some pathogens (Caler et al., 2000; Reddy et al., 2001). In this study, total internal reflection microscopy allowed us to directly visualize a peripheral population of lysosomes (Fig. 2, B and C) that shows calcium-dependent exocytosis (Figs. 3 and 4). This opens the possibility of studying the mechanistic and kinetic details of membrane repair and pathogen invasion. The observation that primary fibroblasts show more extensive calcium induced lysosomal exocytosis than immortalized cultured cells (Fig. 6, A and B; Table III) indicates that a peripheral population of lysosomes that undergoes calcium induced exocytosis is not an aberration of immortalized cell lines in culture. Future studies should clarify if regulated lysosomal exocytosis is more pronounced in primary cells due to its critical role in maintaining plasma membrane integrity under mechanically challenging conditions. In any case, demonstration of a membrane docked pool of lysosomes as the compartment responsible for calcium-induced exocytosis clearly necessitates a revaluation of the physiological functions of this organelle.

Materials and methods

cDNA fusion constructs

pECFP-Golgi and pEYFP-ER were obtained from CLONTECH Laboratories, Inc. Construction of hGH-EGFP (Rivera et al., 2000) Synaptotagmin VII-EGFP (Martinez et al., 2000), CD63-EGFP (Blott et al., 2001), and Rab7-ECFP (Barbero et al., 2002) has been described. VAMP7-ECFP and VAMP8-ECFP were a gift from James Rothman (Sloan Kettering Institute, New York, NY). The plasmids were constructed by inserting the mouse VAMP7 or VAMP8 cDNAs followed by a sequence encoding 3× SGG amino acids into the HindII-AgeI site of the CLONTECH pCFP-N1 vector (CLONTECH Laboratories, Inc.). Lamp1-EGFP was constructed by inserting the rat LGP120 cDNA into the XhoI-EcoRI site of the CLONTECH pEGFP-N2 vector.

Cell treatments

Murine embryonic primary fibroblasts were prepared from day 13.5 embryos of C57BL/6J mice, as described in Tournier et al. (2000), and cultured in DME supplemented with 10% FBS. All experiments were done with cells between passages 1 and 2. CHO fibroblasts, NRK fibroblasts, HeLa cells, MDCK epithelial, CHO and NRK cells were maintained in DME (Mediatech Cellgro) supplemented with 10% FBS, and WM239 melanoma cells were maintained in RPMI (GIBCO BRL) supplemented with 10% FBS, in a 37°C incubator humidified with 5% CO_2. Cells were plated on sterile coverslips (Fisher Scientific) and just before imaging the media was replaced with cell imaging media (CIM; HBSS + 10 mM Hepes + 5% FBS, pH 7.4). Cells were transiently transfected using Lipofectamine 2000 (Invitrogen) or Fugene 6 (Roche) 18–36 h before being imaged. For calcium measurements, CHO cells were loaded for 20 min with 10 μM Fluo-3–AM and 10 μM Fura red–AM, washed three times, and maintained in CIM, after which 10 μM A23187 calcium-ionophore was added (T_{0s}) and the cells were imaged using TIRF microscopy. For calcium ionophore and calcium agonist treatments, growth media was replaced with CIM and mounted on the microscope stage maintained at 37°C. Cells were imaged using TIRFM before and after the addition of 10 μM A23187 ionophore or 0.2 U/ml thrombin or 20 nM bombesin. Calcium ionophore-A23187, thrombin, bombesin and 65 kD TRITC dextran were obtained from Sigma-Aldrich. 10 kD Texas red–dextran and 70 kD FITC dextran were obtained from Molecular Probes, and used to load lysosomes as previously described (Martinez et al., 2000).

Image acquisition

Laser scanning confocal microscopy. Laser scanning confocal microscopy was carried out using a Zeiss LSM 510 confocal microscope using a 63X (Plan-Apochromat, NA 1.40) water immersion objective. GFP was imaged using 488-nm laser light and a 505–530-nm BP emission filter, CFP was imaged using 458-nm laser excitation and 460–500-nm BP emission filter,

Texas red and TRITC were imaged using 543-nm laser excitation and a 580-nm LP emission filter. Serial optical sections were taken using 0.4-μm optical sections.

TIR-FM. The illumination for TIR-FM was done through the objective as previously described (Schmoranzer et al., 2000). It consists of an inverted epifluorescence microscope (IX-70; Olympus) equipped with high numerical aperture lenses (Apo 60X NA 1.45; Olympus) and a home-built temperature-controlled enclosure. GFP tagged proteins were excited with the 488-nm line of an Argon laser (Omnichrome, model 543-AP A01; Melles Griot) reflected off a dichroic mirror (498DCLP). For simultaneous dual-color imaging of GFP/Texas red imaging or Fluo-3/Fura red, we used an emission splitter (W-view; Hamamatsu Photonics). Cells were excited using the 488-nm line of Argon laser. The GFP emission was collected through emission band pass filters (HQ525/50M). The GFP/TR or the Fluo-3/Fura red emissions were collected simultaneously through an emission splitter equipped with dichroic mirrors to split the emission (550DCLP) and emission band pass filters (GFP/Fluo-3, HQ525/50M; TR/Fura red, HQ580LP). All filters were obtained from Chroma Technologies Corp. Images were acquired with a 12-bit cooled CCD ORCA-ER (Hamamatsu Photonics) with a resolution of 1280 × 1024 pixels (pixel size, 6.45 μm^2). The camera and mechanical shutters (Uniblitz, Vincent Associates) were controlled using MetaMorph (Universal Imaging). Images were acquired at 5–10 frames/s. Images containing a region of interest of the cell were streamed to memory on a PC during acquisition and then saved to hard disk. The depth of the evanescent filed was typically ~70–120 nm for the Apo 60× N.A. 1.45 lens (Schmoranzer et al., 2000).

Image processing and quantitative analysis. Processing and analysis of the video sequences was done either with MetaMorph or using in-house software written in LabView. For processing dual-color sequences, the images acquired through the emission splitter such that the separated channels appear side by side on the camera chip were separated, subtracted for background fluorescence, aligned within accuracy of a single pixel using the brightfield or fluorescence images and analyzed using MetaMorph. Finally, the separate channels were pseudo-color encoded and combined in a RGB sequence. Quantitation of fluorescence intensity and (half-[width])^2 was done as described earlier (Schmoranzer et al., 2000).

Online supplemental material

All videos are available at http://www.jcb.org/cgi/content/full/jcb.200208154/DC1. Video 1 corresponds with Fig. 2 C and shows that calcium induces exocytosis of lysosomes in murine embryonic primary fibroblasts. Video 2 corresponds with Fig. 3 D and shows that lysosomal exocytosis leads to the release of both membrane and lumenal content. Video 3 corresponds to Fig. 4 B and shows that calcium induces exocytosis of only a small fraction of lysosomes.

We would like to thank Walther Mothes and Sabyasachi Chakrabarti (Yale University, New Haven, CT) for the Rab7-CFP, and SytVII-GFP, respectively, Anita Reddy (Alexion Pharmaceuticals) for the Lamp 1-GFP, Victor Rivera (ARIAD Pharmaceuticals) for hGH-EGFP, Gillian Griffiths (Oxford University, Oxford, UK) for the CD63-GFP construct, and James Rothman for VAMP7-ECFP and VAMP8-ECFP constructs. We would like to thank Evelyn Voura, Joshua Rapoport, and Jan Schmoranzer for their comments on the manuscript.

This work was supported by National Science Foundation grants BES 0110070 and BES-0119468 to S.M. Simon, and National Institutes of Health grant R01 GM64625 TO N.W. Andrews.

Submitted: 26 August 2002
Revised: 22 October 2002
Accepted: 23 October 2002

References

Advani, R.J., B. Yang, R. Prekeris, K.C. Lee, J. Klumperman, and R.H. Scheller. 1999. VAMP-7 mediates vesicular transport from endosomes to lysosomes. *J. Cell Biol.* 146:765–776.

Andrews, N.W. 2002. Lysosomes and the plasma membrane: trypanosomes reveal a secret relationship. *J. Cell Biol.* 158:389–394.

Axelrod, D. 1981. Cell-substrate contacts illuminated by total internal reflection fluorescence. *J. Cell Biol.* 89:141–145.

Ayala, B.P., B. Vasquez, S. Clary, J.A. Tainer, K. Rodland, and M. So. 2001. The pilus-induced Ca2+ flux triggers lysosome exocytosis and increases the amount of Lamp1 accessible to Neisseria IgA1 protease. *Cell Microbiol.* 3:265–275.

Barbero, P., L. Bittova, and S.R. Pfeffer. 2002. Visualization of Rab9-mediated vesicle transport from endosomes to the trans-Golgi in living cells. *J. Cell Biol.* 156:511–518.

Bennett, J.P., S. Cockcroft, and B.D. Gomperts. 1979. Ionomycin stimulates mast cell histamine secretion by forming a lipid- soluble calcium complex. *Nature.* 282:851–853.

Bi, G.Q., R.L. Morris, G. Liao, J.M. Alderton, J.M. Scholey, and R.A. Steinhardt. 1997. Kinesin- and myosin-driven steps of vesicle recruitment for Ca2+-regulated exocytosis. *J. Cell Biol.* 138:999–1008.

Blott, E.J., and G.M. Griffiths. 2002. Secretory lysosomes. *Nat. Rev. Mol. Cell Biol.* 3:122–131.

Blott, E.J., G. Bossi, R. Clark, M. Zvelebil, and G.M. Griffiths. 2001. Fas ligand is targeted to secretory lysosomes via a proline-rich domain in its cytoplasmic tail. *J. Cell Sci.* 114:2405–2416.

Caler, E.V., D.A. Vaena, P.A. Haynes, N.W. Andrews, and B.A. Burleigh. 1998. Oligopeptidase B-dependent signaling mediates host cell invasion by Trypanosoma cruzi. *EMBO J.* 17:4975–4986.

Caler, E.V., R.E. Morty, B.A. Burleigh, and N.W. Andrews. 2000. Dual role of signaling pathways leading to Ca(2+) and cyclic AMP elevation in host cell invasion by Trypanosoma cruzi. *Infect. Immun.* 68:6602–6610.

Chavez, R.A., S.G. Miller, and H.P. Moore. 1996. A biosynthetic regulated secretory pathway in constitutive secretory cells. *J. Cell Biol.* 133:1177–1191.

Coorssen, J.R., H. Schmitt, and W. Almers. 1996. Ca2+ triggers massive exocytosis in Chinese hamster ovary cells. *EMBO J.* 15:3787–3791.

Eddleman, C.S., M.L. Ballinger, M.E. Smyers, H.M. Fishman, and G.D. Bittner. 1998. Endocytotic formation of vesicles and other membranous structures induced by Ca2+ and axolemmal injury. *J. Neurosci.* 18:4029–4041.

Floto, R.A., M.P. Mahaut-Smith, B. Somasundaram, and J.M. Allen. 1995. IgG-induced Ca2+ oscillations in differentiated U937 cells; a study using laser scanning confocal microscopy and co-loaded fluo-3 and fura-red fluorescent probes. *Cell Calcium.* 18:377–389.

Kendall, J.M., M.N. Badminton, G.B Sala-Newby, A.K. Campbell, and C.M. Rembold. 1996. Recombinant apoaequorin acting as a pseudo-luciferase reports micromolar changes in the endoplasmic reticulum free Ca2+ of intact cells. *Biochem. J.* 318:383–387.

Kornfeld, S., and I. Mellman. 1989. The biogenesis of lysosomes. *Annu. Rev. Cell Biol.* 5:483–525.

Lampson, M.A., J. Schmoranzer, A. Zeigerer, S.M. Simon, and T.E. McGraw. 2001. Insulin-regulated release from the endosomal recycling compartment is regulated by budding of specialized vesicles. *Mol. Biol. Cell.* 12:3489–3501.

Llopis, J., J.M. McCaffery, A. Miyawaki, M.G. Farquhar, and R.Y. Tsien. 1998. Measurement of cytosolic, mitochondrial, and Golgi pH in single living cells with green fluorescent proteins. *Proc. Natl. Acad. Sci. USA.* 95:6803–6808.

Lysakowski, A., H. Figueras, S.D. Price, and Y.Y. Peng. 1999. Dense-cored vesicles, smooth endoplasmic reticulum, and mitochondria are closely associated with non-specialized parts of plasma membrane of nerve terminals: implications for exocytosis and calcium buffering by intraterminal organelles. *J. Comp. Neurol.* 403:378–390.

Marks, M.S., and M.C. Seabra. 2001. The melanosome: membrane dynamics in black and white. *Nat. Rev. Mol. Cell Biol.* 2:738–748.

Martinez, I., S. Chakrabarti, T. Hellevik, J. Morehead, K. Fowler, and N.W. Andrews. 2000. Synaptotagmin VII regulates Ca(2+)-dependent exocytosis of lysosomes in fibroblasts. *J. Cell Biol.* 148:1141–1150.

McNeil, P.L., and R.A. Steinhardt. 1997. Loss, restoration, and maintenance of plasma membrane integrity. *J. Cell Biol.* 137:1–4.

Miyake, K., P.L. McNeil, K. Suzuki, R. Tsunoda, and N. Sugai. 2001. An actin barrier to resealing. *J. Cell Sci.* 114:3487–3494.

Nagamatsu, S., Y. Nakamichi, T. Watanabe, S. Matsushima, S. Yamaguchi, J. Ni, E. Itagaki, and H. Ishida. 2001. Localization of cellubrevin-related peptide, endobrevin, in the early endosome in pancreatic beta cells and its physiological function in exo- endocytosis of secretory granules. *J. Cell Sci.* 114:219–227.

Nagata, T. 2001. Three-dimensional high voltage electron microscopy of thick biological specimens. *Micron.* 32:387–404.

Neylon, C.B., A. Nickashin, P.J. Little, V.A. Tkachuk, and A. Bobik. 1992. Thrombin-induced Ca2+ mobilization in vascular smooth muscle utilizes a slowly ribosylating pertussis toxin-sensitive G protein. Evidence for the involvement of a G protein in inositol trisphosphate-dependent Ca2+ release. *J. Biol. Chem.* 267:7295–7302.

Ninomiya, Y., T. Kishimoto, Y. Miyashita, and H. Kasai. 1996. Ca2+-dependent exocytotic pathways in Chinese hamster ovary fibroblasts revealed by a caged-Ca2+ compound. *J. Biol. Chem.* 271:17751–17754.

Palade, G.E. 1975. Intracellular aspects of the process of protein secretion. *Science.* 189:347–358.

Reddy, A., E.V. Caler, and N.W. Andrews. 2001. Plasma membrane repair is mediated by Ca(2+)-regulated exocytosis of lysosomes. *Cell.* 106:157–169.

Rivera, V.M., X. Wang, S. Wardwell, N.L. Courage, A. Volchuk, T. Keenan, D.A. Holt, M. Gilman, L. Orci, F. Cerasoli, Jr., et al. 2000. Regulation of protein secretion through controlled aggregation in the endoplasmic reticulum. *Science.* 287:826–830.

Rodriguez, A., P. Webster, J. Ortego, and N.W. Andrews. 1997. Lysosomes behave as Ca2+-regulated exocytic vesicles in fibroblasts and epithelial cells. *J. Cell Biol.* 137:93–104.

Schmoranzer, J., M. Goulian, D. Axelrod, and S.M. Simon. 2000. Imaging constitutive exocytosis with total internal reflection fluorescence microscopy. *J. Cell Biol.* 149:23–32.

Sciaky, N., J. Presley, C. Smith, K.J. Zaal, N. Cole, J.E. Moreira, M. Terasaki, E. Siggia, and J. Lippincott-Schwartz. 1997. Golgi tubule traffic and the effects of Brefeldin A visualized in living cells. *J. Cell Biol.* 139:1137–1155.

Steinhardt, R.A., G. Bi, and J.M. Alderton. 1994. Cell membrane resealing by a vesicular mechanism similar to neurotransmitter release. *Science.* 263:390–393.

Stinchcombe, J.C., and G.M. Griffiths. 1999. Regulated secretion from hemopoietic cells. *J. Cell Biol.* 147:1–6.

Togo, T., J.M. Alderton, G.Q. Bi, and R.A. Steinhardt. 1999. The mechanism of facilitated cell membrane resealing. *J. Cell Sci.* 112:719–731.

Tournier, C., P. Hess, D.D. Yang, J. Xu, T.K. Turner, A. Nimnual, D. Bar-Sagi, S.N. Jones, R.A. Flavell, and R.J. Davis. 2000. Requirement of JNK for stress-induced activation of the cytochrome c-mediated death pathway. *Science.* 288:870–874.

Van Lint, J., P. Agostinis, W. Merlevede, and J.R. Vandenheede. 1993. Early responses in mitogenic signaling, bombesin induced protein phosphorylations in Swiss 3T3 cells. *Adv. Enzyme Regul.* 33:143–155.

Zaal, K.J., C.L. Smith, R.S. Polishchuk, N. Altan, N.B. Cole, J. Ellenberg, K. Hirschberg, J.F. Presley, T.H. Roberts, E. Siggia, et al. 1999. Golgi membranes are absorbed into and reemerge from the ER during mitosis. *Cell.* 99:589–601.